[Short title + Author Name - P&H title] 17 (2024) 105809

Contents lists available at ScienceDirect

Arabian Journal of Chemistry

journal homepage: www.ksu.edu.sa

Wuzi Yanzong Pill alleviates spermatogenesis dysfunction by modulating the gut microbial tryptophan metabolites

Juan Liu [a,b], Wuwen Feng [b,c,*], Dandan Zhang [b], Hao Cheng [b], Yaochuan Zhou [b], Jing Wu [b], Zixuan Wang [d], Zhilei Wang [a], Chunyan Fang [a], Guangsen Li [a], Yaodong You [a], Xujun Yu [a,*], Degui Chang [a,*]

[a] TCM Regulating Metabolic Diseases Key Laboratory of Sichuan Province, Hospital of Chengdu University of Traditional Chinese Medicine, Chengdu 610032, China
[b] State Key Laboratory of Southwestern Chinese Medicine Resources, School of Pharmacy, Chengdu University of Traditional Chinese Medicine, Chengdu 611137, China
[c] Key Laboratory of the Ministry of Education for Standardization of Chinese Medicine, Chengdu University of Traditional Chinese Medicine, Chengdu 611137, China
[d] Shanghai Key Laboratory of Complex Prescriptions and MOE Key Laboratory for Standardization of Chinese Medicines, Institute of Chinese Materia Medica, Shanghai University of Traditional Chinese Medicine, Shanghai 201203, China

ARTICLE INFO

Keywords:
Wuzi Yanzong Pill
Spermatogenesis dysfunction
Gut microbiota
Tryptophan metabolites
Energy metabolism

ABSTRACT

Wuzi Yanzong Pill (WZYZP), a classic traditional Chinese medicine prescription, has been widely used to alleviate spermatogenesis dysfunction for hundreds of years. However, the molecular mechanisms of WZYZP treatment for spermatogenesis dysfunction remain limited. Here, our results showed that WZYZP significantly improved spermatogenesis and testicular energy metabolism. The 16S rDNA sequencing showed that WZYZP improved gut microbiota dysbiosis, including increased relative abundances of *Lactobacillus* with the capability of metabolizing Trp. The depletion of gut microbiota by antibiotics suppressed the ability of WZYZP to improve spermatogenesis dysfunction. The untargeted and targeted metabolomics results showed that WZYZP increased Trp metabolites especially aryl hydrocarbon receptor (AhR) ligands. Moreover, WZYZP modulated the AhR/AMPK pathway to improve the expression of spermatogenesis-related genes. The correlation analysis showed that gut microbiota was significantly correlated with Trp metabolites, and Trp metabolites were closely related to spermatogenesis. Overall, the results demonstrated that WZYZP could regulate gut microbiota, and the gut microbial Trp metabolites further act on testicular energy metabolism, thereby indirectly improving spermatogenic dysfunction. Our study provides a novel research strategy for complementary and alternative medicine in male infertility from the perspective of gut microbial metabolites.

1. Introduction

Male infertility is a global health issue affecting approximately 10 – 15 % of couples worldwide, and its prevalence is increasing by 0.291 % per year (Agarwal et al., 2021). Male infertility causes substantial psychological and social distress and imposes a considerable economic

Abbreviations: 3-HAA, 3-hydroxyanthranilic acid; 5-HIAA, 5-hydroxyindole-3-acetic acid; 5-HTP, 5-Hydroxytryptophan; AhR, aryl hydrocarbon receptor; *Ahr*, aryl-hydrocarbon receptor; AMPKα, AMP-activated protein kinase alpha; ATP, adenosine triphosphate; *Cyp1a1*, cytochrome P450 family 1 subfamily A member 1; *Cyp1b1*, cytochrome P450 family 1 subfamily B member 1; *Dmc1*, DNA meiotic recombinase 1; GAPDH, glyceraldehyde-3-phosphate dehydrogenase; GLUT1, glucose transporter 1; H&E, hematoxylin-eosin; I3CA, indole-3-carboxylic acid; IA, indole-3-acrylic acid; IAA, indole-3-acetic acid; IAId, indole-3-carboxaldehyde; IAM, indole-3-acetamide; IND, indole; ILA, indole-3-lactic acid; IPA, indole-3-propionic acid; Kyn, kynurenine; LDHA, lactate dehydrogenase A; MCT4, monocarboxylate transporter 4; OTUs, operational taxonomic units; p-AMPKα, phospho-AMP-activated protein kinase alpha; PCoA, principal coordinates analysis; *Plzf*, promyelocytic leukemia zinc finger; qRT-PCR, quantitative real-time polymerase chain reaction; SCs, Sertoli cells; SD, standard deviation; SPF, specific pathogen-free; *Str8*, stimulated by retinoic acid 8; *Sycp3*, synaptonemal complex protein 3; TCM, traditional Chinese medicine; Trp, tryptophan; WZYZP, Wuzi Yanzong Pill; WZYZP-H, high dose of Wuzi Yanzong Pill; WZYZP-H-Abx, high dose of Wuzi Yanzong Pill with antibiotics; WZYZP-L, low dose of Wuzi Yanzong Pill; WZYZP-M, middle dose of Wuzi Yanzong Pill.

* Corresponding authors at: State Key Laboratory of Southwestern Chinese Medicine Resources, School of Pharmacy, Chengdu University of Traditional Chinese Medicine, Chengdu 611137, China. (W. Feng). TCM Regulating Metabolic Diseases Key Laboratory of Sichuan Province, Hospital of Chengdu University of Traditional Chinese Medicine, Chengdu 610032, China (D. Chang, X. Yu).

E-mail addresses: jiaoxiake-1@foxmail.com (W. Feng), 20639179@qq.com (X. Yu), changdegui123@163.com (D. Chang).

https://doi.org/10.1016/j.arabjc.2024.105809
Received 12 November 2023; Accepted 23 April 2024
Available online 24 April 2024

burden on patients (Agarwal et al., 2021). Spermatogenesis is crucial to maintaining male fertility, and the disturbance of spermatogenesis in the testis is regarded as one of the main causes of male infertility (Chen et al., 2021). A study examining the trend of sperm count among men showed that the worldwide decline of sperm count is continuing in the 21st century at an accelerated pace (Levine et al., 2023). Although treatments such as hormonal drug therapy, surgical intervention, and assisted reproductive technology have been widely used to treat male spermatogenesis disorders, they are expensive and may have adverse effects (Jiang et al., 2017). Therefore, it is of great value to find other suitable medicines for the treatment of male spermatogenesis disturbance.

Wuzi Yanzong Pill (WZYZP), originally recorded in "Xuanjie Lu" in the Tang Dynasty, is a classic Chinese medicine formula composed of *Lycium barbarum* L., *Plantago asiatica* L., *Schisandra chinensis* (Turcz.) Baill., *Cuscuta chinensis* Lam, and *Rubus chingii* Hu (Ji et al., 2016). It has been used to treat male infertility with the properties of kidney nourishing and essence strengthening in China for a long time (Chen et al., 2021). Recent clinical studies have shown that WZYZP can safely and effectively improve semen quality in patients with oligospermia (Yong et al., 2020; Zhao et al., 2018). In addition, *in vitro* and *in vivo* experiments confirmed the protective effect of WZYZP on experimental spermatogenesis disorders (Chen et al., 2021; Wu et al., 2023). However, our understanding of the molecular mechanisms underlying WZYZP for the treatment of spermatogenesis dysfunction remains limited.

The gut microbiota is an essential regulator of host physiology and health, affecting various aspects of body functions including male reproduction (Liu et al., 2022; Wang et al., 2024). Accumulating data from human and animal studies has shown the association between gut microbiota composition and male fertility potential, including sperm quantity and quality, hormonal regulation, and testicular function (Ding et al., 2020; Zhang et al., 2021; Zhang et al., 2022). Small molecules produced by gut microbiota, including tryptophan (Trp) metabolites, vitamins, bile acids, and short-chain fatty acids, serve as important intermediates between microbiota and testis to maintain spermatogenesis (Wang et al., 2023a; Yan et al., 2022; Zhang et al., 2022). Notably, studies have shown that orally administered TCM components with low oral bioavailability can modulate these metabolites to exert therapeutic effects (Juan et al., 2018). For example, kaempferol with low oral bioavailability can exert anti-arthritic effects by rebalancing gut microbiota and its metabolites, including Trp, fatty acid, and secondary bile acid (Aa et al., 2020). The ingredients of WZYZP include polysaccharides, flavonoids, alkaloids, and other ingredients with low oral bioavailability (Zou et al., 2015). Therefore, this study aims to investigate the possible mechanism of WZYZP improving spermatogenesis disorder from the perspective of gut microbiota and its metabolites.

Herein, the ameliorative effect of WZYZP on spermatogenesis was investigated in cyclophosphamide-induced spermatogenic dysfunction mice. Then, the effect of WZYZP on the gut microbiota was explored via 16S rDNA sequencing. We further performed antibiotic treatment to investigate whether the ameliorating effect of WZYZP on impaired spermatogenesis depends on the presence of gut microbiota. We also investigated the effect of WZYZP on gut microbiota metabolites by non-target and targeted metabolomics analysis. To further explore the possible mechanism of WZYZP regulating gut microbial Trp metabolites to improve spermatogenesis, we detected the expression of AhR target genes such as *Cyp1a1* and *Cyp1b1*, protein expression related to AhR/AMPK pathway, and expression level of spermatogenesis-related genes including *Plzf*, *Dmc1*, *Sycp3*, and *Stra8* in testicular tissues. In addition, we performed the integrative analysis of the relations among specific gut microbiota, Trp metabolites, phenotypes, and their associated genes to understand the potential mechanisms of WZYZP for spermatogenesis dysfunction.

2. Materials and methods

2.1. Drugs and materials

Wuzi Yanzong Pill (WZYZP, a water honey pill) was purchased from Beijing Tong Ren Tang Co., Ltd. (Beijing, China). Cyclophosphamide was purchased from Jiangsu Hengrui Medicine Co., Ltd. (Jiangsu, China). Neomycin, ampicillin, metronidazole, and vancomycin were purchased from Shanghai Yuanye Bio-Technology Co., Ltd. (Shanghai, China). Hyperoside, verbascoside, kaempferol, and schisandrin were purchased from Shanghai Yuanye Bio-Technology Co., Ltd. (Shanghai, China).

2.2. Chemical components analysis and quality control of WZYZP

The chemical components of WZYZP were analyzed by UPLC-QTOF-MS. To ensure the quality of WZYZP, high-performance liquid chromatography (HPLC) was used to quantitatively analyze the contents of hyperoside, verbascoside, kaempferol, and schisandrin in WZYZP according to the 2020 edition of Chinese Pharmacopoeia. The detailed methods were provided in the Supplementary methods.

2.3. Animals and WZYZP administration

Specific pathogen-free (SPF)-grade adult male Kunming mice (8 weeks old, 32 − 38 g) were purchased from Chengdu Dossy Experimental Animal Co., Ltd. (Chengdu, China). Animals were housed under the SPF conditions with a temperature of 22 ± 2 °C, a relative humidity of 60 ± 5 %, and a standard 12 h/12 h light/dark cycle. All animal experiments were approved by the Ethics Committee of Chengdu University of Traditional Chinese Medicine (CDUTCM-2022116) and it was carried out following the National Institutes of Health Guidelines for Care and Use of Laboratory Animals.

After 1 week of acclimatization, mice were randomized into five groups (n = 6): the control group, model group, WZYZP-L group, WZYZP-M group, and WZYZP-H group. Except for the control group, the other groups of mice were injected with cyclophosphamide at a dose of 60 mg/kg/d for 5 days to induce spermatogenic dysfunction. In detail, cyclophosphamide was dissolved in 0.9 % NaCl and injected intraperitoneally into the mice (60 mg cyclophosphamide/kg body weight), once a day for 5 days (Chi et al., 2022). The mice in the control group were injected intraperitoneally with 0.9 % NaCl (0.01 ml/g/d) for 5 days in the same manner. Then, in the WZYZP-L, WZYZP-M, and WZYZP-H groups, concerning previous studies, mice were treated with WZYZP at doses of 0.35 g/kg/d, 0.70 g/kg/d, and 1.40 g/kg/d by gavage for 14 days, respectively (Chen et al., 2021). The mice in the control and model groups were given sterile water in the same manner for 14 days. Before the end of the experiment, feces were collected, snap-frozen in liquid nitrogen, transferred, and stored at − 80 °C for the analysis of gut microbiota and fecal metabolomics. At the end of the trial, all mice were fasted overnight (12 h) and anesthetized by intraperitoneal injection of 2 % pentobarbital (50 mg/kg). The plasma was obtained by centrifugation at 3,000 revolutions per minute (rpm) at 4 °C for 15 min and stored at − 80 °C for the determination of testosterone, pyruvate, lactate, and adenosine triphosphate, as well as the analysis of tryptophan metabolism. The testis and epididymis were immediately excised, and the testis was weighed for counting testicular index (i.e., total testicular weight/body weight). The left testis further was photographed. The left epididymis was cut into pieces for sperm count and motility measurement. The right epididymis and left testis used for histopathological analysis were fixed in 4 % paraformaldehyde. The remaining testis were frozen at − 80 °C for further biochemical analysis, including assay kits and Western blotting.

2.4. Sperm count and motility measurement

The cauda epididymis was minced in 500 μL PBS (pH 7.2) and incubated at 37 °C for 5 min to release the sperm. Sperm motility and sperm count were analyzed using a Digital Color Sperm Quality Detection System (WLJY-9000, Beijing, China).

2.5. Histological examination

The testis and epididymis were fixed in 4 % paraformaldehyde for 24 h, dehydrated in graded ethanol, embedded in paraffin, and sectioned at 4 μm in thicknesses. The sections of the testis and epididymis were stained with hematoxylin-eosin (H&E) and observed under a pathological section scanner (NanoZoomer S60, Hamamatsu, Japan).

2.6. Plasma and testicular testosterone assay

The concentrations of testosterone in the plasma and the testis for each mouse were assayed using commercially available enzyme immunoassay kits specific for mice (CSB-E05101m, Cusabio, Wuhan, China).

2.7. Determination of pyruvate, lactate, and adenosine triphosphate (ATP)

The levels of testicular pyruvate, lactate, and ATP were detected using the commercially available kit (Nanjing Jiancheng Bioengineering Institute, Nanjing, China) according to the manufacturer's protocol.

2.8. Gut microbiota analysis

Total bacterial DNA was extracted from feces using an E.Z.N.A.® soil kit (Omega Bio-Tek, Norcross, GA, U.S.) according to the manufacturer's protocol. DNA was amplified with Gene Amp 9700 PCR system (Applied Biosystems, Singapore) using barcoded universal bacterial primers targeting variable region V3-V4 of 16SrRNA gene with 338F-806R barcoded primers: 338 Forward Primer (5′-ACTCCTACGGGAGGCAGCAG-3′), 806 Reverse Primer (5′-GGACTACHVGGGTWTCTAAT-3′). The amplification system includes 10 ng of template DNA, 4 μL FastPfu buffer, 2 μL dNTPs (2.5 nM), 0.8 μL forward primer (5 μM), and 0.8 μL reverse primer (5 μM). The PCR conditions were as follows: initial denaturation at 95 °C for 3 min, followed by 27 cycles of denaturation at 95 °C for 30 s, annealing at 55 °C for 30 s, and extension at 72 °C for 30 s, with a final extension at 72 °C for 10 min. Each PCR was performed in triplicate, then combined, and quality checked on an agarose gel. Each PCR amplification was then quantified using QuantiFluor™-ST (Promega, USA), and each sample was pooled into an equal amount of 200 ng to form a library. Sequencing was performed on an Illumina MiSeq PE300 platform (Illumina, San Diego, USA) in Shanghai Majorbio Biopharm Technology Co., Ltd. (Shanghai, China).

2.9. Antibiotics (Abx) treatment

After a week of adaptation, 12 mice were randomly divided into the WZYZP-H group (n = 6) and WZYZP-H with antibiotics (WZYZP-H-Abx) group (n = 6). All 12 mice were injected with cyclophosphamide at a dose of 60 mg/kg/d for 5 days to induce spermatogenic dysfunction (Chi et al., 2022). Then, mice in the WZYZP-H and WZYZP-H-Abx groups were treated with WZYZP at doses of 0.70 g/kg/d by gavage for 14 days. Meanwhile, mice in the WZYZP-H group and the WZYZP-H-Abx group were given sterile water and water with Abx for 14 days, respectively. The antibiotics cocktail was composed of 0.5 mg/mL of neomycin, 0.5 mg/mL of ampicillin, 0.5 mg/mL of metronidazole, and 0.125 mg/mL of vancomycin provided in the drinking water changed twice per week (Zhao et al., 2023).

2.10. Untargeted metabolomics analysis of feces by UPLC-QTOF-MS

Metabolomics profiling of fecal samples of mice was performed at Shanghai Majorbio Bio-pharm Technology Co., Ltd. (Shanghai, China). Briefly, 50 mg of feces were homogenized with 100 μL water for 3 min. Then, an aliquot of 400 μL of methanol-containing internals standard was mixed with feces to extract the metabolites. The homogenized sample was centrifuged at 13,000 *g* and 4 °C for 15 min. The supernatant was transferred to a 200 μL vial for UPLC-Q-TOF/MS analysis. The chromatographic separations were carried on an ACQUITY UPLC® HSS T3 column (1.8 μm, 100 mm × 2.1 mm). The mobile phase was composed of solvent A (acetonitrile/water, 5:95, *v/v*, containing 0.1 % formic acid) and solvent B (isopropanol/acetonitrile/water, 47.5:47.5:5, *v/v/v*, containing 0.1 % formic acid). The gradient elution condition was as follows: 100 % A (0 − 0.5 min), 100 %−75 % A (0.5 − 2.5 min), 75 %−0% A (2.5 − 9 min), 0 % A (9 − 13 min), 100 % A (13 − 13.1 min), 100 % A (13.1 − 16 min). The column temperature and flow rate were set at 40 °C and 400 μL/min, respectively. The sample injection volume was 10 μL.

The ESI source conditions were set as follows: the positive and negative ESI spray voltages at 5.0 kV and 4.0 kV, respectively; and ion source temperature at 550 °C. Both the sheath gas and the auxiliary gas were nitrogen. The sheath gas pressure was 30 psi, and the auxiliary gas pressure was 50 psi. The parameters of the full mass scan were as follows: a resolution of 70,000, a maximum isolation time of 50 ms, a normalized collision energy of 30 v, and an *m/z* range of 50 − 1,000. Data were collected and processed with Progenesis QI (Waters Corp., Milford, USA).

2.11. Targeted metabolomics analysis of plasma by UHPLC-QTRAP-MS

The mouse blood samples were centrifuged at 3,000 rpm and 4 °C for 15 min, and the supernatants were collected. Targeted Trp metabolomics in plasma were determined by LC-ESI-MS/MS (UHPLC-QTRAP). Briefly, 80 μL plasma was mixed with 360 μL methanol (containing the internal standards), vortexed, and ultrasound at low temperature for 30 min (5 °C, 40 kHz). After centrifugation at 13,500 rpm and 4 °C for 15 min, the supernatant was freeze-dried in a freeze dryer. Re-dissolved plasma samples (1 % of acetonitrile, containing 0.1 % formic acid) were further vortexed and centrifuged. The supernatant was then injected into the UPLC-MS/MS system. Samples were injected into an ACQUITY UPLC® HSS T3 column (1.8 μm, 150 mm × 2.1 mm) at a flow rate of 0.35 mL/min. The column temperature was set at 40 °C. The sample injection volume was 2 μL. The mobile phase was composed of solvent A (water, containing 0.1 % formic acid) and solvent B (acetonitrile, containing 0.1 % formic acid). The gradient elution condition was as follows: 99 %−89 % A (0 − 2.5 min), 89 % A (2.5 − 5.5 min), 89 %−72 % A (5.5 − 6.5 min), 72 % A (6.5 − 7.5 min), 72 %−50 % A (7.5 − 12.5 min), 50 %−5% A (12.5 − 13.5 min), 5 %A (13.5 − 15.5 min), 5 %−99 % A (15.5 − 15.6 min), 99 % A (15.6 − 18 min). QTRAP 6500 + mass spectrometer was operated in positive and negative polarity mode with a positive ion spray voltage of 5,500 V and a negative ion spray voltage of 4,000 V.

2.12. Quantitative real-time PCR analysis

Total RNA was extracted from the testis using a total RNA isolation kit (RNAqueous®, Invitrogen). Reverse transcription cDNA synthesis and quantitative real-time polymerase chain reaction (qRT-PCR) analysis were performed as described. The relative expression of mRNA was detected by the $2^{-\Delta\Delta Ct}$ method (Wu et al., 2023). The forward and reverse primers of the detected genes are shown in Table S1.

2.13. Western blotting analysis

The testicular tissues were lysed with RIPA buffer (Servicebio,

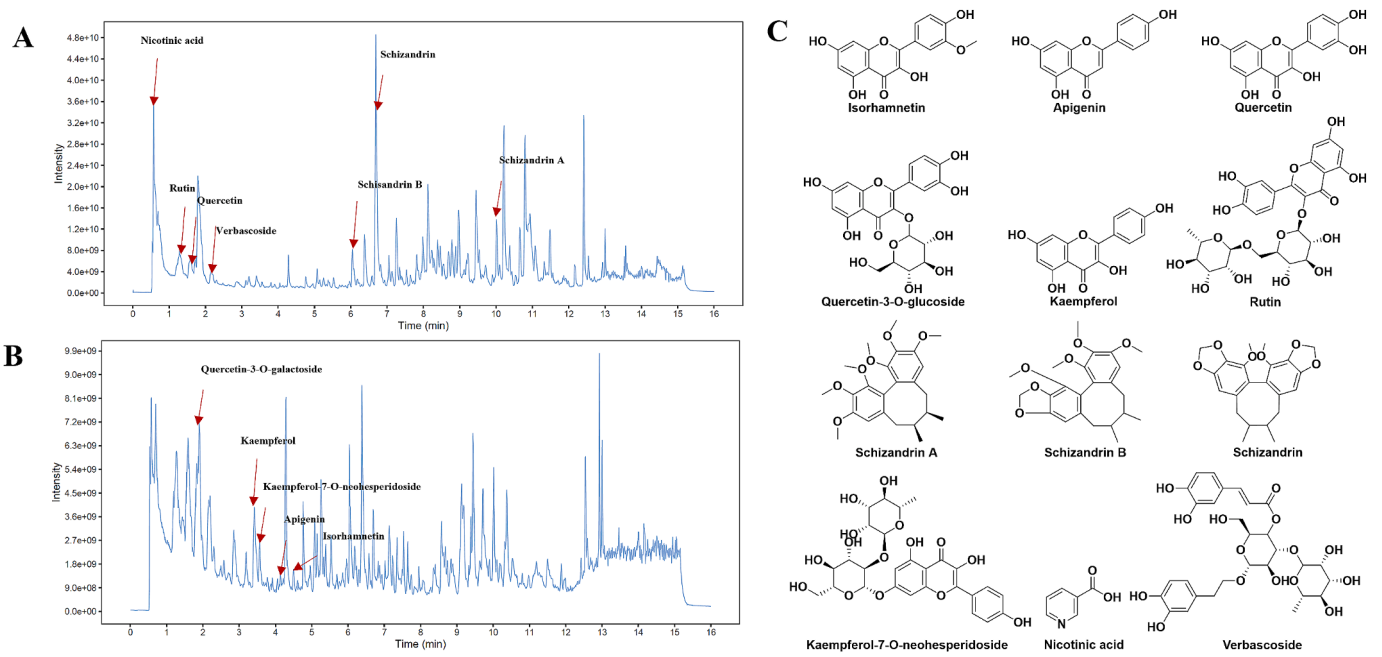

Fig. 1. Analysis of the chemical components of the WZYZP by UPLC-Q-TOF/MS. (A, B) Total ion chromatography of WZYZP in (A) positive and (B) negative ion modes. (C) The typical structures of the main bioactive compounds.

Wuhan, China) to obtain total protein. Total protein concentration was measured by BCA Protein Assay kit (Servicebio, Wuhan, China), followed by protein denaturation. The equal amounts of denatured total protein from each sample were then loaded onto 8 % or 10 % SDS-PAGE (Servicebio, Wuhan, China) for separation and transferred to PVDF (Merck Millipore, Darmstadt, Germany). Subsequently, the membranes were blocked with 5 % skimmed milk (Servicebio, Wuhan, China) at room temperature for 1 h and incubated overnight at 4 °C with primary antibodies anti-AhR (1:1,000, ABclonal, A1451), anti-AMPKα (1:1,000, ABclonal, A12718), anti-p-AMPKα-Thr172 (1:1,000, ZEN-BIOSCIENCE, R381164), anti-GLUT1 (1:1,000, ABclonal, A11727), anti-LDHA (1:1,000, ZEN-BIOSCIENCE, R24822), anti-MCT4 (1:1,000, ABclonal, A3016), anti-GAPDH (1:1,000, Servicebio, GB15004) and anti-β-Actin (1:1,000, Servicebio, GB15003). Later, the membranes were incubated with secondary antibody anti-rabbit IgG (1:3,000, Servicebio, GB23303) for 1.5 h at room temperature. The protein band in membranes was visualized using an enhanced chemiluminescence reagent (Westernblot, Beijing, China) in the Bio-Rad ChemiDoc MP imaging system (Hercules, CA, USA).

2.14. Statistics

Data were expressed as mean ± standard deviation (SD). Statistical analysis was performed in GraphPad Prism version 8.02. Unpaired two-tailed student's *t*-test was used to compare two different groups, and one-way ANOVA with Dunnett's multiple comparison test was performed to compare more than two groups. Differences with $P < 0.05$ were considered to be statistically significant.

3. Results

3.1. Chemical component identification and quality control of WZYZP

The chemical profile of WZYZP was analyzed by UPLC-Q/TOF-MS using the positive and negative ion models. In total, 52 compounds were identified, including flavonoids, alkaloids, phenylpropanoids, and organic acids (Table S2 and Fig. 1A–B), such as quercetin, kaempferol, quercetin-3-O-galactoside, isorhamnetin, apigenin, rutin, schizandrin A, verbascoside (Fig. 1C). Many of these compounds are reported to exhibit low oral bioavailability, such as quercetin, kaempferol, and rutin (Aa et al., 2020; Feng et al., 2019), suggesting WZYZP may act indirectly on hosts to treat diseases. Further, the levels of key components were determined by HPLC. Fig. S1A and B displayed the chromatograms of the mixed reference solution and WZYZP, respectively. The levels of major components in the WZYZP (compared to the weight of WZYZP) were hyperoside (0.379 mg/g), verbascoside (0.152 mg/g), kaempferol (0.161 mg/g), and schisandrin (0.136 mg/g). The results met the requirements of Chinese Pharmacopoeia (Committee of National Pharmacopoeia, 2020).

3.2. WZYZP improved spermatogenesis and energy metabolism

As shown in Fig. 2E, the testis index was significantly increased in groups of WZYZP-L, WZYZP-M, and WZYZP-H compared with the model group. Similarly, compared with the model group, WZYZP treatment significantly increased the testis size in a dose-dependent manner (Fig. 2A). H&E staining of testis showed that WZYZP significantly increased the number of spermatogenic cells and the thickness of the seminiferous epithelium in a dose-dependent manner (Fig. 2B). Furthermore, epididymal H&E staining showed a small amount of mature sperm in the model group, but the number of mature sperm was notably increased by WZYZP in a dose-dependent manner (Fig. 2C). Similarly, all three WZYZP treatment groups significantly increased sperm concentration, sperm motility, as well as testicular and plasma testosterone concentrations compared with the model group (Fig. 2D–I). Since energy plays an important role in spermatogenesis (Rato et al., 2012), we further examined the contents of pyruvate, lactate, and ATP in testicular tissue. Compared with the model group, WZYZP significantly reversed the decrease of pyruvate, lactate, and ATP in a dose-dependent manner (Fig. 2J–L). Taken together, these results demonstrated that WZYZP significantly improved spermatogenesis and energy metabolism in mice with spermatogenesis dysfunction.

3.3. WZYZP improved spermatogenesis dysfunction in a gut microbiota–dependent manner

The gut microbiota plays a vital role in spermatogenesis (Zhang et al., 2021), therefore, we analyzed the changes of the gut microbiome

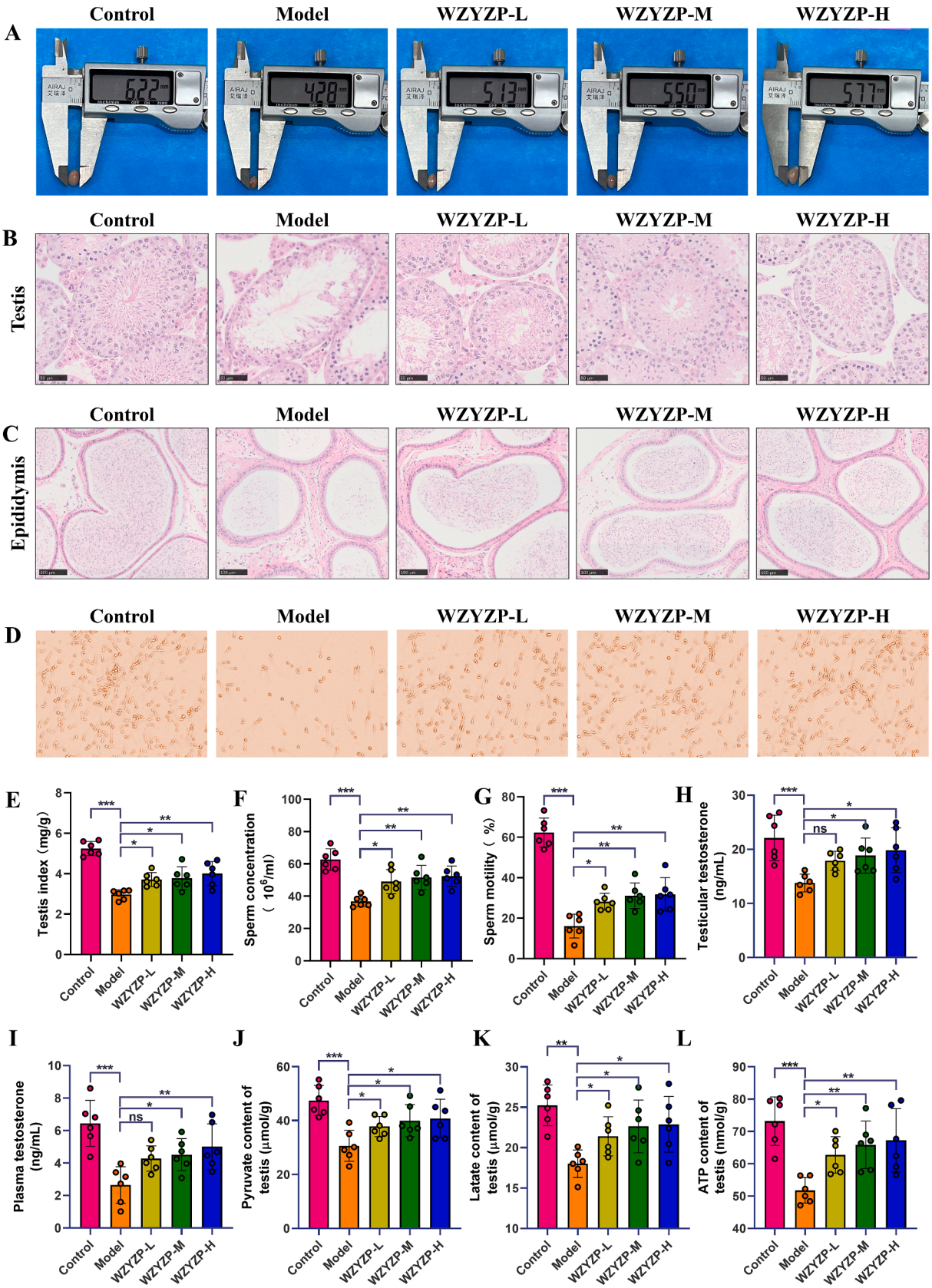

Fig. 2. The effects of WZYZP on spermatogenesis and energy metabolism. (A) Morphology of the testis. (B) The representative testicular sections with H&E staining (magnification = × 400, scale bar = 50 μm). (C) The representative epididymal sections with H&E staining (magnification = × 200, scale bar = 100 μm). (D) The representative pictures of sperm morphology and quantity. (E) Testis index of mice in each group. (F) Sperm concentration and (G) motility of mice in each group. (H, I) Testosterone levels in testis (H) and plasma (I). (J) Expression of testicular pyruvate. (K) Expression of testicular lactic acid. (L) Expression of testicular ATP. Data were shown as mean ± SD. *$P < 0.05$, **$P < 0.01$, ***$P < 0.001$, and ns represents no significant difference.

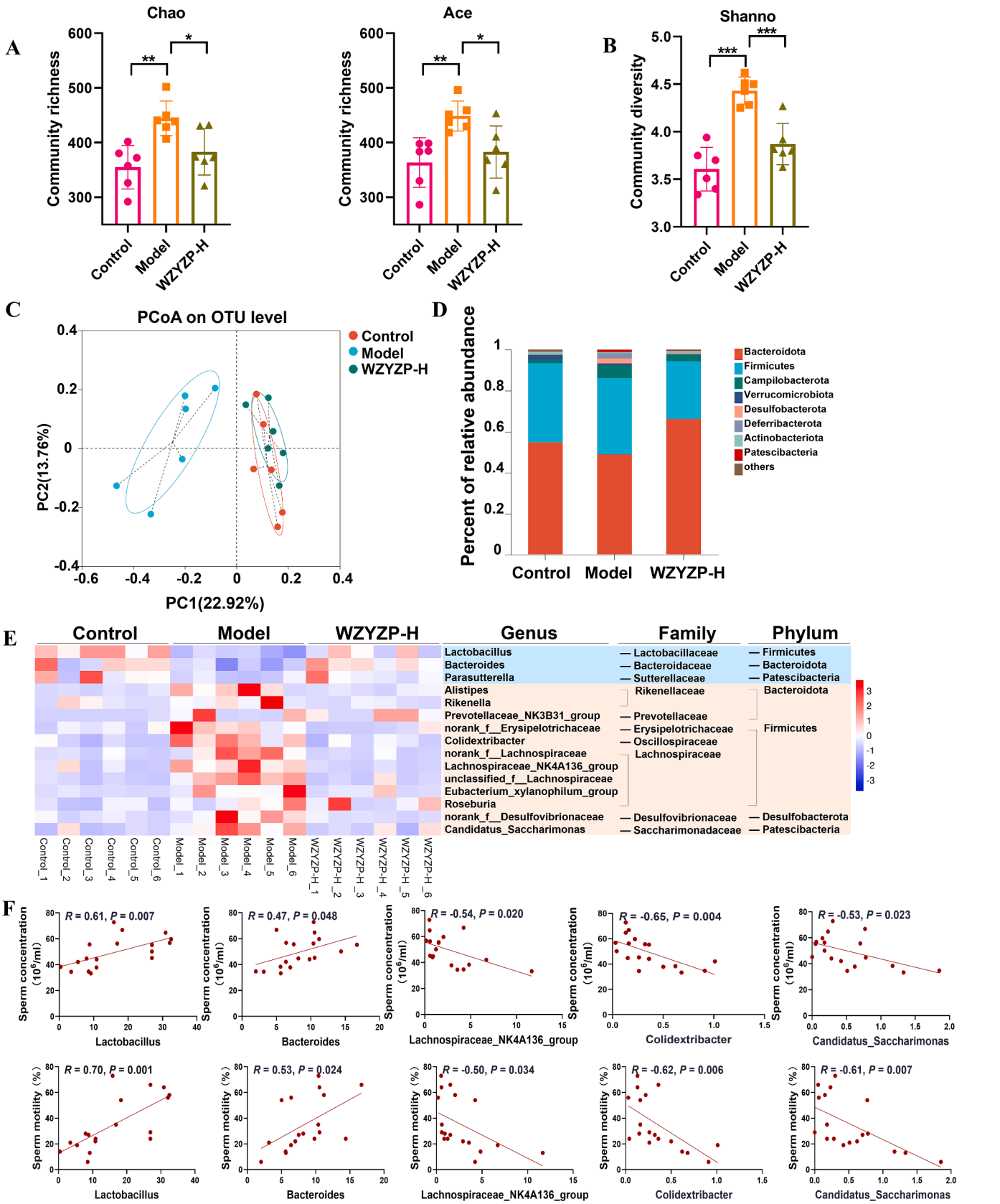

Fig. 3. The effects of WZYZP-H on the gut microbiota. (A) The richness and (B) diversity of gut microbiota. (C) Principal coordinate analysis (PCoA) plot of gut microbiota based on the operational taxonomic units (OTUs) abundance. (D) Bacterial taxonomic profiling at the phylum level of gut microbiota. (E) Heatmap of differential gut microbiota abundance among control, model, and WZYZP-H groups. The color of the spots in the left panel represents the relative abundance of the genus level in each group. (F) Spearman's correlation analysis of the gut microbiota of genus level with sperm concentration and motility. Data were shown as mean ± SD. $^{*}P < 0.05$, $^{**}P < 0.01$, and $^{***}P < 0.001$.

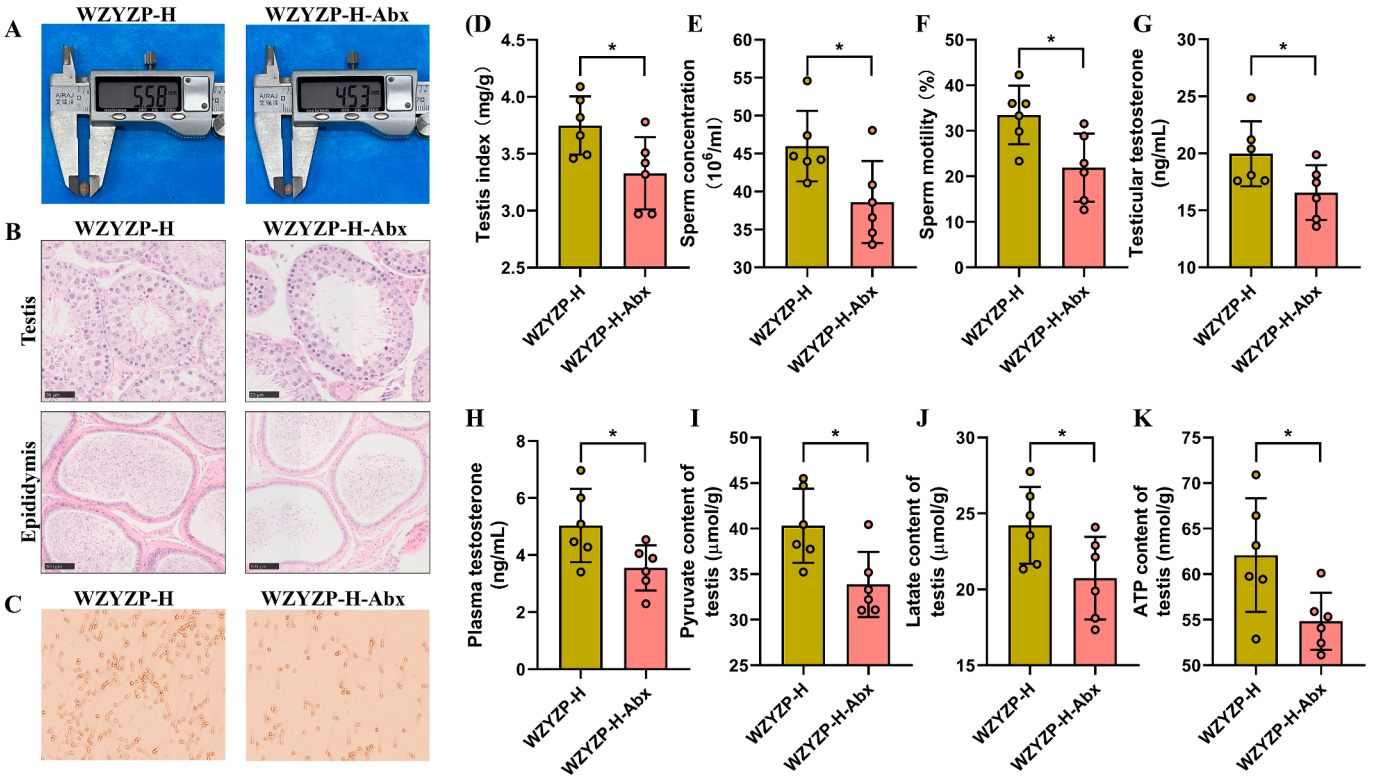

Fig. 4. Effect of antibiotic-induced microbiota depletion on WZYZP-H in improving spermatogenesis. (A) Morphology of the testis. (B) The representative H&E staining of testicular sections (magnification = × 400, scale bar = 50 μm) and epididymal sections (magnification = × 200, scale bar = 100 μm). (C) The representative pictures of sperm morphology and quantity. (D) Testis index of mice. (E) Sperm concentration and (F) motility of mice. (G, H) Testosterone levels in testis (G) and plasma (H). (I) Levels of testicular pyruvate in mice. (J) Levels of testicular lactic acid in mice. (K) Levels of testicular ATP in mice. Data were shown as mean ± SD. *$P < 0.05$.

after the WZYZP-H intervention. As revealed in Fig. 3A–B, the Chao index, Ace index, and Shannon index of gut microbiota were significantly altered, indicating that the richness and diversity of the gut microbiota were reduced in the WZYZP-H group. A distinct clustering of gut microbiota composition in the control group, model group, and WZYZP-H group was observed using principal coordinates analysis (PCoA) (Fig. 3C). Moreover, the clustering of gut microbiota in WZYZP-H group was closer to that of the control group (Fig. 3C). The phylum level of gut microbiota indicated that the relative abundances of Bacteroidota and Proteobacteria were decreased and Desulfobacterota and Patescibacteria were increased in the model group compared with the control group, while WZYZP-H significantly restored these levels (Fig. 3D and Fig. S2A).

We further analyzed the change of gut microbiota at the genus level, in which fifteen bacteria were altered in the control, model, and WZYZP-H groups (Fig. 3E). Most of these changed bacteria belonged to phyla Firmicutes and Bacteroidota. Among these genus-level bacteria, the relative abundances of *Lactobacillus* and *Bacteroides* were significantly decreased in the model group compared with the control group, while WZYZP-H significantly increased these levels (Fig. S2B). Moreover, the relative abundances of *Lachnospiraceae_NK4A136_group*, *Colidextribacter*, and *Candidatus_Saccharimonas* were significantly decreased by WZYZP-H treatment (Fig. S2B). The Spearman's correlation showed that genera *Lactobacillus* and *Bacteroides* were positively while genera *Lachnospiraceae_NK4A136_group*, *Colidextribacter*, and *Candidatus_Saccharimonas* were negatively correlated with the sperm concentration and motility (Fig. 3F).

To investigate whether the ameliorating effect of WZYZP on impaired spermatogenesis depends on the presence of gut microbiota, we treated mice in the WZYZP-H group with a cocktail of antibiotics (Abx) containing metronidazole, neomycin, vancomycin, and ampicillin to deplete gut microbiota (Zhao et al., 2023). After Abx treatment, the OTUs of gut microbiota in the WZYZP-H-Abx group (48) were significantly lower than those in the WZYZP-H group (2183), which is equivalent to 97.9 % reduction in OTUs (Fig. S3A). Moreover, the alpha diversity of gut microbiota and the vast majority of the gut microbiota at genus levels were significantly reduced by Abx treatment (Fig. S3B–D). These results suggested that the Abx protocol efficiently depleted the majority of gut microbiota in our study. Importantly, the depletion of gut microbiota suppressed the ability of WZYZP-H to improve spermatogenesis dysfunction (Fig. 4A–K). These findings indicated that the ameliorating effect of WZYZP on impaired spermatogenesis acted in a gut microbiota-dependent manner.

3.4. *WZYZP modulated fecal microbial metabolites*

Since the fecal metabolome, a functional readout of the gut microbiota, is considered an intermediate phenotype mediating interactions between host and microbes (Zierer et al., 2018), we investigated the changes of fecal metabolites in mice after treatment with WZYZP-H by untargeted metabolomics. The partial least squares discriminant analysis (PLS-DA) score plot showed a distinct clustering of fecal metabolites between control and model groups, as well as the model and WZYZP-H groups in positive ion mode (Fig. S4A–D). Moreover, PLS-DA showed that WZYZP-H treatment showed a trend to shift toward the control group (Fig. S4E–F). Compared with the control group, 133 metabolites were significantly altered in the model group, of which 83 metabolites were significantly reduced and 50 metabolites were significantly increased (Fig. 5A). Compared with the model group, 101 metabolites were significantly changed in the WZYZP-H group, of which 42 metabolites were significantly decreased and 59 metabolites were significantly increased (Fig. 5B). However, only 22 metabolites changed

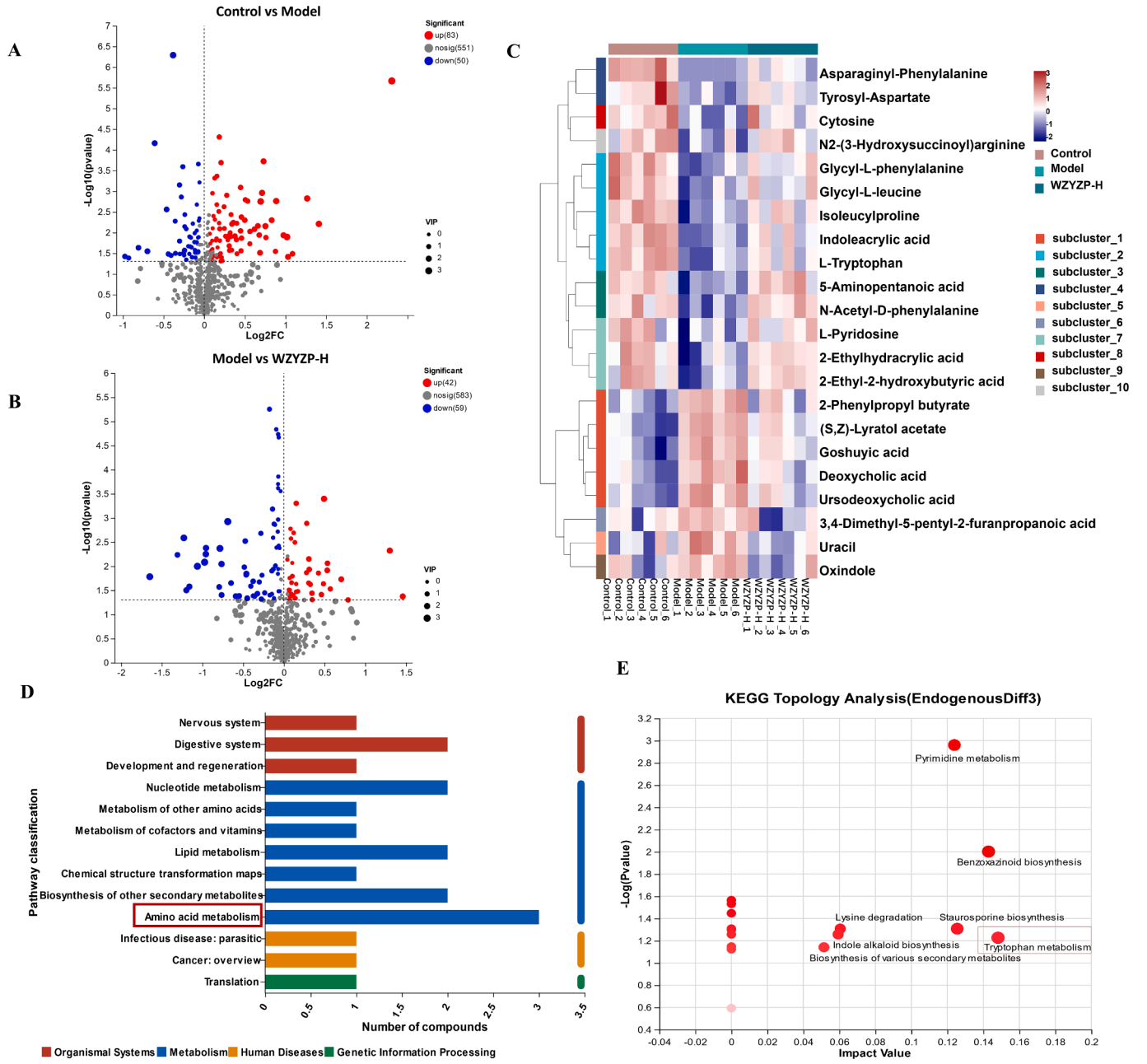

Fig. 5. The effects of WZYZP-H on the fecal metabolites. (A) Volcano plot of differential metabolites between control and model groups. (B) Volcano plot of differential metabolites between model and WZYZP-H groups. (C) Heatmap showing the relative abundances of differential metabolites in fecal samples. (D) The functional annotation of differential metabolites in fecal samples. (E) Key altered pathway of differential metabolites with metabolomics pathway analysis (MetPA).

significantly between the control and the model and could be significantly reversed by WZYZP-H (Fig. 5C, Table S3). To investigate the functional information of the 22 differential metabolites in the feces regulated by WZYZP-H, we performed functional annotation of KEGG pathway. KEGG pathway functional annotation showed that the differential metabolites have the highest distribution ratio in the amino acid metabolism (Fig. 5D). The KEGG pathway enrichment analysis displayed that tryptophan metabolism was the most important metabolic pathway (impact value: 0.148) (Fig. 5E). These results suggested that WZYZP-induced tryptophan metabolism may play an important role in improving spermatogenesis.

3.5. *WZYZP modulated microbial tryptophan metabolism*

Given that microbial metabolites entering the host blood circulation is an important way for gut microbiota to have a functional impact on the host pathophysiology (Koh and Bäckhed, 2020), we further performed targeted detection of the Trp metabolite levels in the plasma of mice. We observed a decreased level of Trp in the model group compared to the control group, while WZYZP-H significantly increased the concentration of Trp compared to the model group (Fig. 6A). As for indole and its derivatives, the concentrations of indole-3-lactic acid (ILA, Fig. 6B), indole-3-acrylic acid (IA, Fig. 6C), indole-3-propionic acid (IPA, Fig. 6D), indole (IND, Fig. 6E), indole-3-carboxylic acid (I3CA, Fig. 6F), indole-3-acetamide (IAM, Fig. 6G), indole-3-acetic acid (IAA, Fig. 6H), indole-3-carboxaldehyde (IAId, Fig. 6I) were lower in the model group than that of the control group. After WZYZP-H treatment, the concentrations of indole and its derivatives in model mice were increased (Fig. 6B–I). Among these derivatives, IA, IAA, and IAId are ligands of aryl hydrocarbon receptor (AhR) and they originate from the

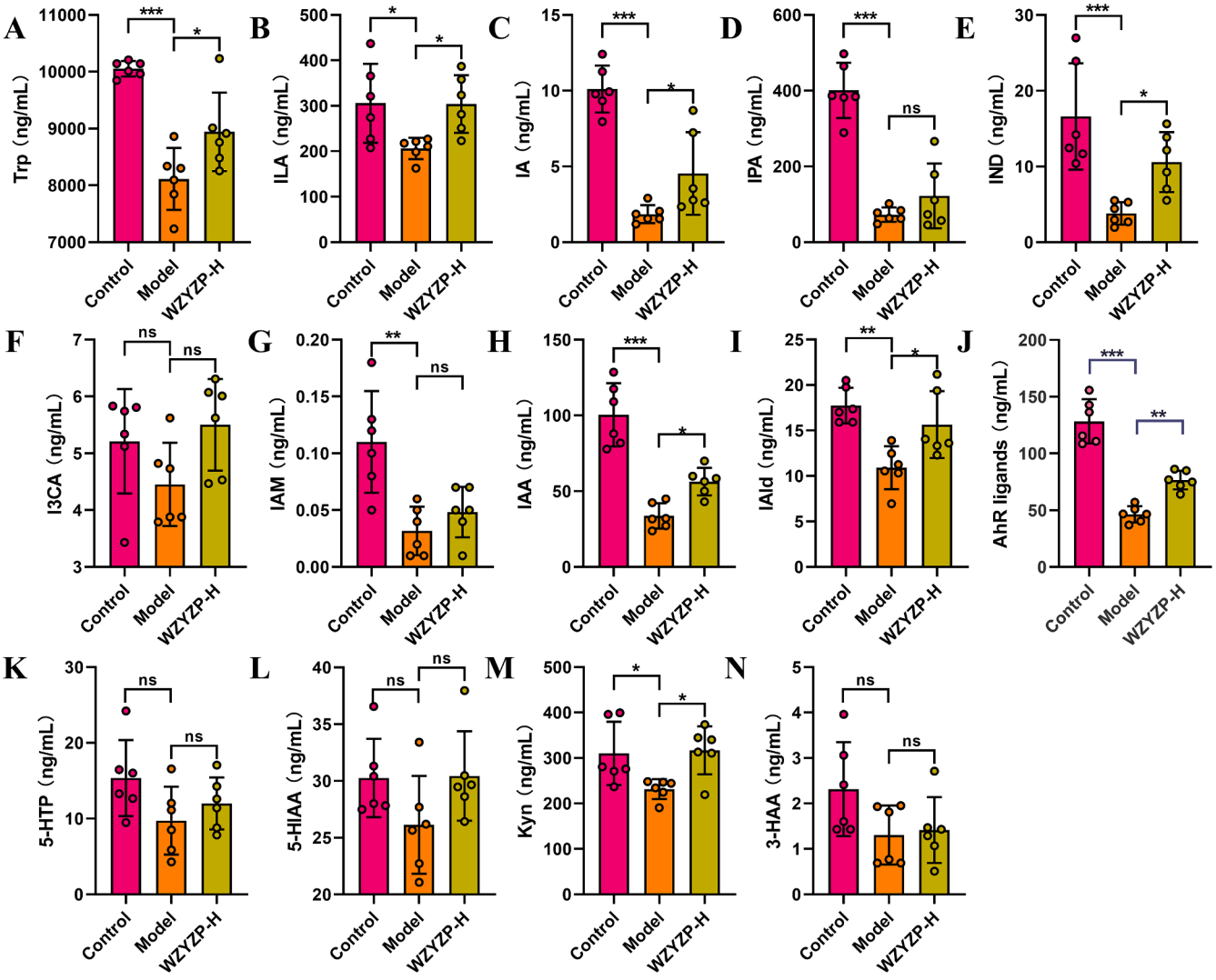

Fig. 6. The effects of WZYZP-H on tryptophan metabolites. Quantification of tryptophan metabolites, (A) Trp, (B) ILA, (C) IA, (D) IPA, (E) IND, (F) I3CA, (G) IAM, (H) IAA, (I) IAId, (J) AhR ligands, (K) 5-HTP, (L) 5-HIAA, (M) Kyn, and (N) 3-HAA in plasma from mice. Data were shown as mean ± SD. $^{*}P < 0.05$, $^{**}P < 0.01$, $^{***}P < 0.001$, and ns represents no significant difference.

metabolism of Trp by microbe (Agus et al., 2018). Notably, there were significant reductions in ligands of AhR in the model group, compared with the control group, while WZYZP-H treatment significantly attenuated these reductions (Fig. 6J). The 5-hydroxytryptophan (5-HTP) production pathway and kynurenine (Kyn) pathway are the other two metabolism pathways of Trp. Metabolites corresponding to the Kyn pathway were decreased in the model group and were significantly increased by WZYZP-H, while 5-HTP pathway-related metabolites including 5-hydroxyindole-3-acetic acid (5-HIAA), and 3-hydroxyanthranilic acid (3-HAA) were not significantly altered (Fig. 6K–N). Taken together, these findings demonstrated that WZYZP treatment facilitated the conversion of Trp towards AhR ligands in mice with spermatogenesis dysfunction.

3.6. *WZYZP modulated the AhR/AMPK pathway to improve spermatogenesis*

Studies have shown that AhR activation by AhR ligands can activate the AMP-activated protein kinase (AMPK) (Muku et al., 2019). Moreover, AMPK regulates adenosine triphosphate (ATP) through the glycolytic pathway, which is critical for the energy requirements of spermatogenesis (Xie et al., 2022). Thus, we detected AhR activation, protein expression related to the AhR/AMPK pathway, and expression level of spermatogenesis-related genes in testicular tissues. It was shown that *Ahr* gene expression was suppressed in the model group, and was significantly increased by WZYZP-H (Fig. 7A). Furthermore, we observed an increase in the expressions of the *Ahr* transcriptional targets *Cyp1a1* and *Cyp1b1* in the WZYZP-H group compared to that of the model group (Fig. 7B, C). WZYZP-H significantly reversed the decrease of AhR protein expression (Fig. 7D, E). Meanwhile, the protein expression level of p-AMPKα was significantly increased in the WZYZP-H group compared to that of the model group (Fig. 7D, F). Similarly, GLUT1, LDHA, and MTC4 expression levels were significantly elevated after WZYZP-H treatment in comparison to the model group (Fig. 7G, H). In addition, similar outcomes were obtained in the expression level of spermatogenesis-related genes in testicular tissues. As shown in Fig. 7I, the expression level of *Plzf*, which is essential for spermatogonia self-renewal (Hobbs et al., 2010), was significantly up-regulated in the WZYZP-H group compared with the model group. Other genes, including *Dmc1*, *Sycp3*, and *Stra8*, well-known markers of spermatocyte meiosis (Liu et al., 2022), were significantly increased by WZYZP-H treatment (Fig. 7I). Together, these results suggested that WZYZP-H improved spermatogenesis dysfunction possibly via regulation of the AhR/AMPK pathway.

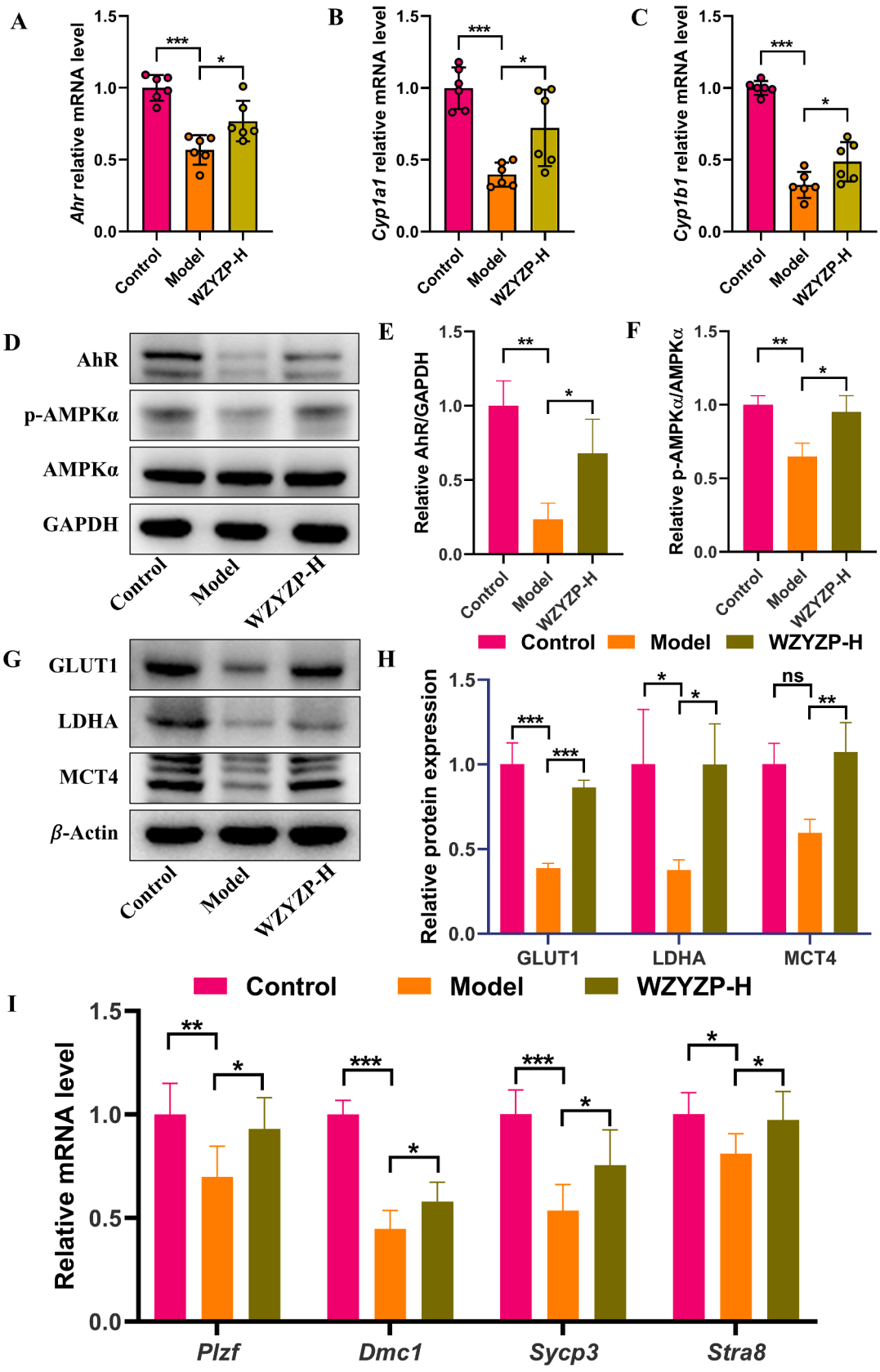

Fig. 7. WZYZP modulated AhR/AMPK pathway to improve spermatogenesis. Relative mRNA expressions of (A) *Ahr*, (B) *Cyp1a1*, and (C) *Cyp1b1* in the testis. (D) Representative Western blotting bands and quantitation of (E) AhR, (F) p-AMPKα protein expression in the testis. (G) Representative Western blotting bands and quantitation of (H) GLUT1, LDHA, MCT4 protein expression in the testis. (I) Relative mRNA expressions of spermatogenesis-related genes, including *Plzf*, *Dmc1*, *Sycp3*, and *Stra8* in the testis. Data were shown as mean ± SD. $^{*}P < 0.05$, $^{**}P < 0.01$, $^{***}P < 0.001$, and ns represents no significant difference.

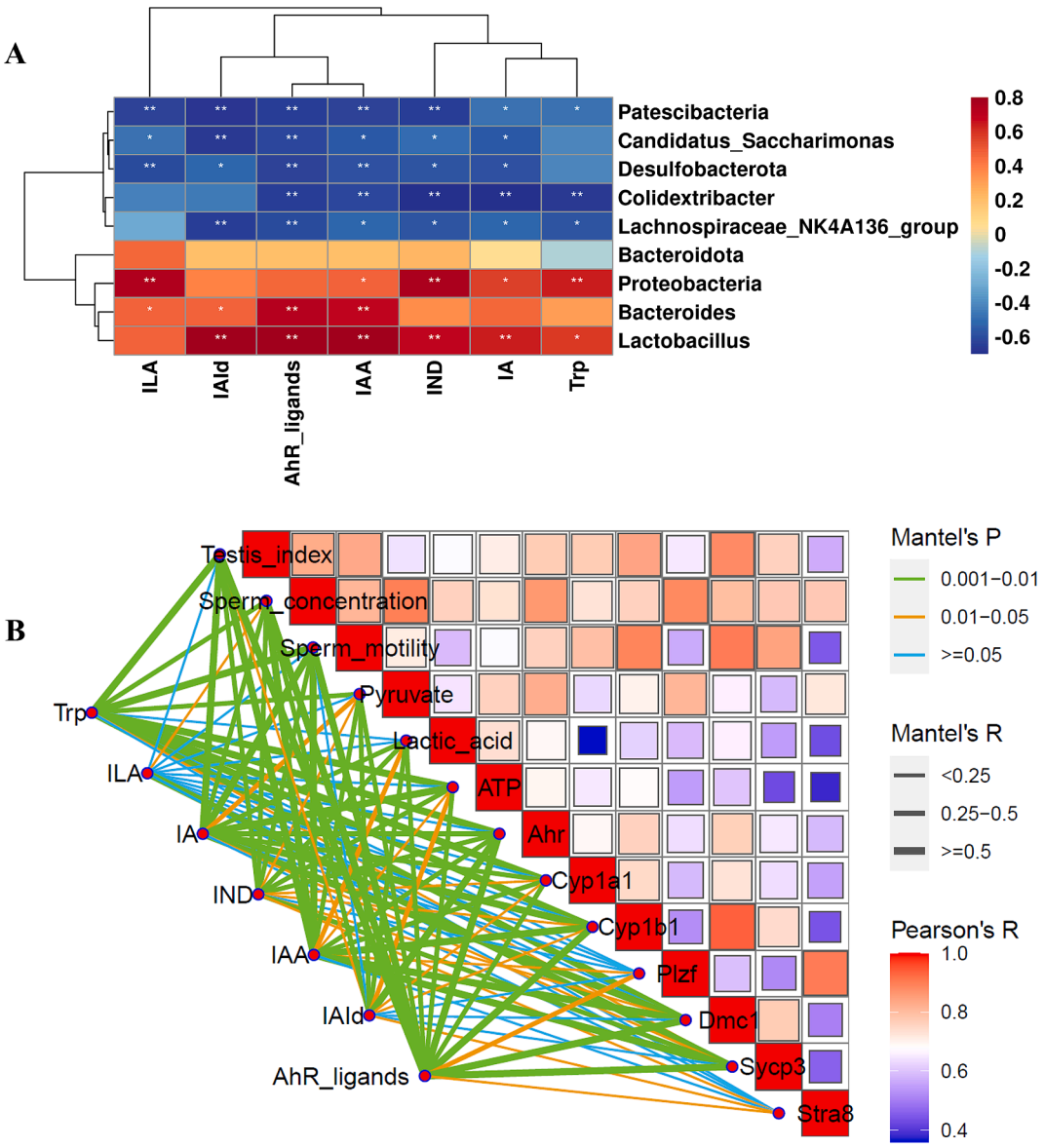

Fig. 8. Association map of the three-tiered analyses integrating the gut microbiota, Trp metabolites, and phenotypes as well as their associated genes. (A) Heat maps of the Spearman rank correlation coefficient and significant tests between the differential bacteria and Trp metabolites. (B) Pairwise comparisons of phenotypes and their associated genes, with a color gradient denoting Spearman's correlation coefficient. Trp metabolites were related to phenotypes and their associated genes by partial (geographic distance–corrected) Mantel tests. Edge width corresponds to the Mantel's R statistic for the corresponding distance correlations, and edge color denotes the statistical significance based on 9,999 permutations.

3.7. Integrated mechanism of WZYZP on spermatogenesis dysfunction

To further explore the relationship between the WZYZP-H-induced changes in gut microbiota composition and gut microbial Trp metabolites, we performed Spearman rank correlation. As shown in Fig. 8A, four bacterial strains (phyla Bacteroidota and Proteobacteria, genera *Lactobacillus* and *Bacteroides*) were positively while five bacterial strains (phylum Desulfobacterota Patescibacteria, genera *Lachnospiraceae_NK4A136_group*, *Colidextribacter*, and *Candidatus_Saccharimonas*) were negatively correlated with ILA, IAId, AhR ligands, IAA, IND, and IA. Moreover, most of the correlations between the gut microbiota and AhR ligands (including IA, IAA, and IAId) were significant (Fig. 8A). We further performed the Mantel test to explore the relationship among the WZYZP-H-induced changes in Trp metabolites, AhR-related targets, and functional genes related to spermatogenesis. The results showed a significant correlation between Trp metabolites (including AhR ligands, IAA, IA, and Trp) and the gene expression levels of *Ahr*, *Cyp1a1*, and *Cyp1b1* (Mantel's $r > 0.25$, Mantel's $P < 0.05$, Fig. 8B), indicating AhR activation is potentially correlated with Trp metabolites. Moreover, AhR activation (*Ahr*, *Cyp1a1*, and *Cyp1b1*) was significantly positively correlated with energy metabolism (pyruvate, lactic acid, and ATP) (Fig. 8B). The energy metabolism (pyruvate, lactic acid, and ATP) was significantly positively correlated with spermatogenesis-related genes (*Plzf*, *Dmc1*, and *Sycp3*) (Fig. 8B). Additionally, spermatogenesis-related genes (*Plzf*, *Dmc1*, and *Sycp3*) were positively correlated with sperm concentration (Fig. 8B). Taken together, these results showed the intrinsic relationship that WZYZP improved spermatogenesis impairment through gut microbial Trp metabolites.

4. Discussion

The metabolism and bioenergetics of testicular cells are well known for their unique characteristics. Sertoli cells (SCs) are the only somatic cells in the seminiferous tubule of the testis that are in direct and close

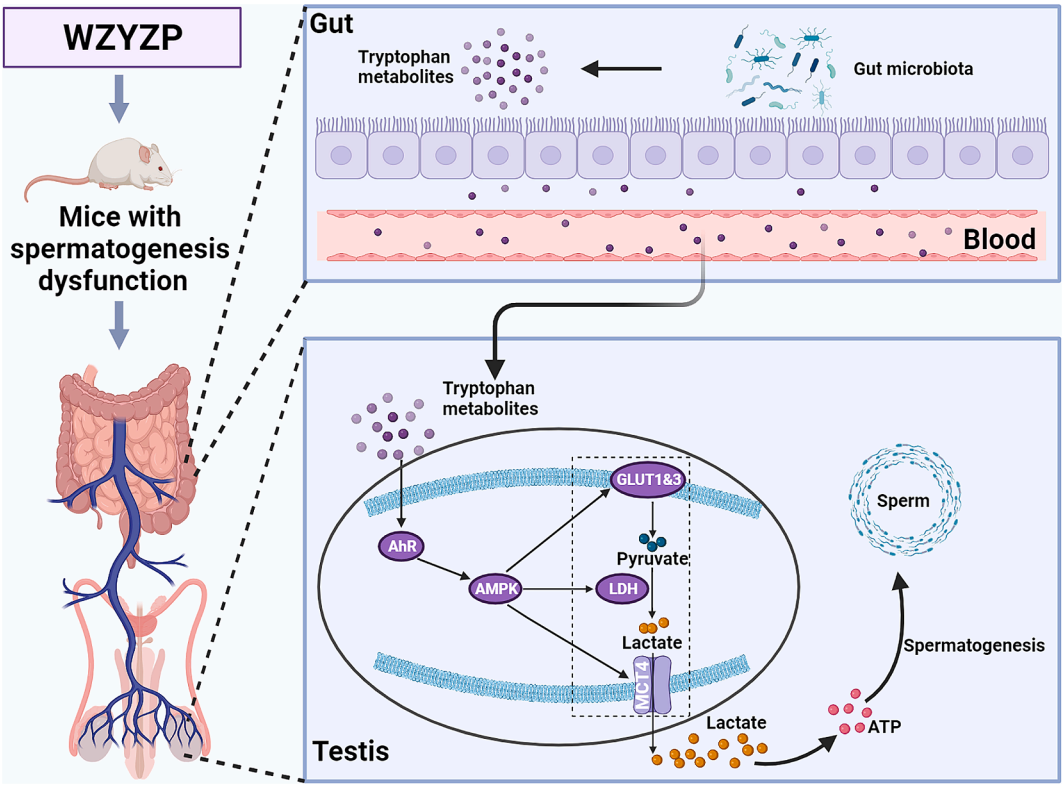

Fig. 9. WZYZP alleviated spermatogenesis dysfunction by modulating the gut microbial tryptophan metabolites.

contact with the germ cells, materially providing the energy and nutritional support required for spermatogenesis (Ni et al., 2019). SCs are considered to be the major energy regulators of spermatogenesis because they can metabolize various substrates, preferentially glucose uptake from the circulation, the majority of which is converted to lactate for developing germ cells (Rato et al., 2012). Conversely, spermatogenesis dysfunction can occur when the germ cells do not receive sufficient energy (Rato et al., 2012). Thus, the concentrations of pyruvate, lactate, and ATP in testicular tissue were examined in this study. In this study, pyruvate, lactate, and ATP were significantly decreased in the model group compared with the control group, which was consistent with the report of energy deficiency in rats with impaired spermatogenesis (Luo et al., 2020). Moreover, the levels of pyruvate, lactate, and ATP in the testis were increased by WZYZP. These results indicated that the improvement of spermatogenesis dysfunction by WZYZP was related to the regulation of glycolysis.

Gut microbiota has been linked to spermatogenesis dysfunction (Ding et al., 2020; Sun et al., 2022). A shift toward a decrease in Bacteroidota and Proteobacteria was identified in mice with spermatogenesis dysfunction (Ding et al., 2020; Sun et al., 2022). Here we showed that WZYZP significantly increased Bacteroidota and Proteobacteria. Interestingly, we also found that WZYZP significantly reduced Desulfobacterota compared with the model group. Until now, Desulfobacterota has not been reported in association with spermatogenesis dysfunction whether in humans or animals. However, some studies have found that the overgrowth of Desulfobacterota is associated with intestinal inflammatory diseases, obesity, and diabetes (Li et al., 2022; Wang et al., 2023b; Wu et al., 2021). Therefore, Desulfobacterota may be a candidate bacterium for predicting spermatogenesis dysfunction and male infertility. At the genus level, *Lactobacillus* and *Bacteroides* were significantly increased by WZYZP in mice with spermatogenesis dysfunction. *Lactobacillus* has previously been reported in normal sperm samples (Baud et al., 2019), and has been shown to improve sperm quality, including increasing sperm count and motility (Darwish et al., 2022). Consistent with previous findings, the results of correlation analysis in our study showed that *Lactobacillus* was positively associated with both sperm count and sperm motility in mice with spermatogenesis dysfunction. The results consistent with previous reports suggest the importance of these bacteria in improving spermatogenesis.

Metabolomes are essential for understanding microbiota-host metabolic dialogues (Chaudhari et al., 2021). Here, WZYZP modulated microbial Trp metabolism. Trp metabolism in the gut involves the direct conversion of Trp by the gut microbiota into several molecules, such as IND and its derivatives(Agus et al., 2018). Many IND derivatives, such as IA, IAA, IAId, and indole-3-acetaldehyde (IAAId), are ligands of AhR (Alexeev et al., 2018; Hubbard et al., 2015). Only a few commensal species with the capability of producing AhR ligands, such as *Lactobacillus* spp and *Peptostreptococcus Russell* (Lamas et al., 2016; Wlodarska et al., 2017) have been identified. *Lactobacillus* was significantly increased by WZYZP treatment. In addition, Spearman analysis showed that IA, IAA, and IAId were significantly positively correlated with *Lactobacillus*. Thus, the increased levels of ligands of AhR, including IA, IAA, and IAId, may be attributed to increased abundances of *Lactobacillus*.

Alterations in Trp metabolites have been observed to be associated with spermatogenesis dysfunction (Fan et al., 2022). Among them, some IND derivatives produced by the decomposition of Trp via gut microbiota are the major endogenous ligands for AhR, which is a ligand-activated transcription factor and an important regulator for maintaining energy homeostasis, including energy metabolism of germ cells in testis (Pohjanvirta, 2017; Shi et al., 2022). AhR activation can regulate the activity of AMPK (Kim et al., 2022). Activation of AMPK increases glucose uptake and lactate production by upregulating GLUT1, LDH, and MCT4 in SCs to ensure lactate supply for spermatogenesis (Galardo et al., 2010). In the present study, WZYZP treatment increased the protein expression levels of AhR, p-AMPKα, GLUT1, LDHA, and MTC4 of the testis. In addition, the concentrations of pyruvate, lactate, and ATP in the testis that increased by WZYZP treatment were significantly

correlated with spermatogenesis-related genes (*Plzf*, *Dmc1*, and *Sycp3*). These results demonstrated that WZYZP-regulated Trp metabolites may activate AhR, further promoting glycolysis through AMPK activation to produce energy for spermatogenesis.

In addition to oral bioavailability, the blood-testis barrier plays a key role in the efficacy of drugs that act on the testis. The cells of the blood-testis barrier express a variety of drug transport enzymes that can pump drugs out of the testis, such as P-glycoprotein, multidrug resistance-related proteins, etc., making it difficult for exogenous drugs to enter the testis (Mruk et al., 2011). Nevertheless, the blood-testis barrier still allows some substances to enter the testes, especially amino acids, glucose, nucleosides, and other substances with nutritional effects (Mruk et al., 2011). Most of the chemical compounds of TCMs show low oral bioavailability and they are hard to penetrate the blood-testis barrier (Jiang et al., 2018; Shiao et al., 2017). However, to our knowledge, no study has noticed the conundrum between remarkable efficacy and low bioavailability of TCMs acting on the testis. The chemical analysis results showed that WZYZP mainly contains flavonoids, alkaloids, phenylpropanoids, etc. Most of these compounds show low oral bioavailability and are hard to enter the testis. Therefore, we hypothesize that the original compounds in WZYZP may act indirectly on the testis. Other studies have proved that gut microbial metabolites IND and IND derivatives can pass through the blood-testis barrier and act as AhR ligands to activate AhR, which further promotes spermatogenesis (Tufek and Yahyazadeh, 2021; Wang and Xie, 2022). In our study, we found out that WZYZP increased plasma levels of AhR ligands IND and IND derivatives. We also detected elevated expression of AhR and increased activation of AhR in the testis. Therefore, WZYZP can act indirectly on testis to improve spermatogenesis via upregulating gut microbial Trp metabolites. Thus, our study provides an answer for the mechanism of natural compounds acting on the testis, i.e., natural compounds can modulate gut microbiota metabolites, which can easily enter the testis, to indirectly achieve efficacy.

5. Conclusion

In conclusion, our findings demonstrate that WZYZP improved spermatogenesis dysfunction, and its therapeutic mechanism is associated with shaping the gut microbiota composition and increasing the gut microbial Trp metabolites, which further increased energy metabolism of spermatogenesis through the AhR/AMPK pathway (Fig. 9). Our study provides a novel research strategy for complementary and alternative medicine in spermatogenesis dysfunction and male infertility.

CRediT authorship contribution statement

Juan Liu: Conceptualization, Funding acquisition, Investigation, Methodology, Validation, Visualization, Writing – original draft. **Wuwen Feng:** Conceptualization, Funding acquisition, Methodology, Writing – review & editing. **Dandan Zhang:** Investigation, Methodology, Software. **Hao Cheng:** Investigation. **Yaochuan Zhou:** Investigation. **Jing Wu:** Investigation. **Zixuan Wang:** Conceptualization. **Zhilei Wang:** Investigation. **Chunyan Fang:** Investigation. **Guangsen Li:** Resources. **Yaodong You:** Resources. **Xujun Yu:** Resources, Supervision. **Degui Chang:** Resources, Supervision.

Declaration of Competing Interest

The authors declare that they have no known competing financial interests or personal relationships that could have appeared to influence the work reported in this paper.

Acknowledgments

This work was supported by the National Natural Science Foundation of China (No. 82104409, 82304850), the National Interdisciplinary Innovation Team of Traditional Chinese Medicine (ZYYCXTD-D-202209), the China Postdoctoral Science Foundation (No. 2023MD734103) and the Sichuan Science and Technology Program (No. 2023NSFSC1778).

Appendix A. Supplementary data

Supplementary data to this article can be found online at https://doi.org/10.1016/j.arabjc.2024.105809.

References

Aa, L.X., Fei, F., Qi, Q., Sun, R.B., Gu, S.H., Di, Z.Z., Aa, J.Y., Wang, G.J., Liu, C.X., 2020. Rebalancing of the gut flora and microbial metabolism is responsible for the anti-arthritis effect of kaempferol. Acta Pharmacol. Sin. 41, 73–81.
Agarwal, A., Baskaran, S., Parekh, N., Cho, C.L., Henkel, R., Vij, S., Arafa, M., Selvam, M. K.P., Shah, R., 2021. Male infertility. The Lancet. 397, 319–333.
Agus, A., Planchais, J., Sokol, H., 2018. Gut microbiota regulation of tryptophan metabolism in health and disease. Cell Host Microbe. 23, 716–724.
Alexeev, E.E., Lanis, J.M., Kao, D.J., Campbell, E.L., Kelly, C.J., Battista, K.D., Gerich, M. E., Jenkins, B.R., Walk, S.T., Kominsky, D.J., 2018. Microbiota-derived indole metabolites promote human and murine intestinal homeostasis through regulation of interleukin-10 receptor. Am. J. Pathol. 188, 1183–1194.
Baud, D., Pattaroni, C., Vulliemoz, N., Castella, V., Marsland, B.J., Stojanov, M., 2019. Sperm microbiota and its impact on semen parameters. Front. Microbiol. 10, 234.
Chaudhari, S.N., McCurry, M.D., Devlin, A.S., 2021. Chains of evidence from correlations to causal molecules in microbiome-linked diseases. Nat. Chem. Biol. 17, 1046–1056.
Chen, W.Q., Wang, B., Ding, C.F., Wan, L.Y., Hu, H.M., Lv, B.D., Ma, J.X., 2021. In vivo and in vitro protective effects of the Wuzi Yanzong pill against experimental spermatogenesis disorder by promoting germ cell proliferation and suppressing apoptosis. J. Ethnopharmacol. 280, 114443.
Chi, Y.N., Ye, R.J., Yang, J.M., Hai, D.M., Liu, N., Ren, J.W., Du, J., Lan, X.B., Yu, J.Q., Ma, L., 2022. Geniposide attenuates spermatogenic dysfunction via inhibiting endoplasmic reticulum stress in male mice. Chem. Biol. Interact. 366, 110144.
Committee of National Pharmacopoeia, Pharmacopoeia of People's Republic of China (I), Chemical Industry Press, Beijing, 2020, 641−642.
Darwish, A., Khattab, A.E.N., Sharaf, H., Abdelhafez, M., El-Razik, A., 2022. Improvement of male mice fecundity by using two new lactobacillus strains. Egypt. J. Chem. 65, 317–321.
Ding, N., Zhang, X., Di Zhang, X., Jing, J., Liu, S.S., Mu, Y.P., Peng, L.L., Yan, Y.J., Xiao, G.M., Bi, X.Y., 2020. Impairment of spermatogenesis and sperm motility by the high-fat diet-induced dysbiosis of gut microbes. Gut. 69, 1608–1619.
Fan, Y., Xu, Q., Qian, H., Tao, C., Wan, T., Li, Z., Yan, W., Niu, R., Huang, Y., Chen, M., 2022. High-fat diet aggravates prenatal low-dose DEHP exposure induced spermatogenesis disorder: characterization of testicular metabolic patterns in mouse offspring. Chemosphere. 298, 134296.
Feng, W., Ao, H., Peng, C., Yan, D., 2019. Gut microbiota, a new frontier to understand traditional Chinese medicines. Pharmacol. Res. 142, 176–191.
Galardo, M., Riera, M., Pellizzari, E., Sobarzo, C., Scarcelli, R., Denduchis, B., Lustig, L., Cigorraga, S., Meroni, S., 2010. Adenosine regulates Sertoli cell function by activating AMPK. Mol. Cell. Endocrinol. 330, 49–58.
Hobbs, R.M., Seandel, M., Falciatori, I., Rafii, S., Pandolfi, P.P., 2010. Plzf regulates germline progenitor self-renewal by opposing mTORC1. Cell. 142, 468–479.
Hubbard, T.D., Murray, I.A., Perdew, G.H., 2015. Indole and tryptophan metabolism: endogenous and dietary routes to ah receptor activation. Drug Metab. Dispos. 43, 1522–1535.
Ji, H.J., Wang, D.M., Wu, Y.P., Niu, Y.Y., Jia, L.L., Liu, B.W., Feng, Q.J., Feng, M.L., 2016. Wuzi Yanzong pill, a Chinese polyherbal formula, alleviates testicular damage in mice induced by ionizing radiation. BMC Complement. Altern. Med. 16, 1–7.
Jiang, D., Coscione, A., Li, L., Zeng, B.Y., 2017. Effect of Chinese herbal medicine on male infertility. Int. Rev. Neurobiol. 135, 297–311.
Jiang, Z., Zhou, B., Li, X., Kirby, G.M., Zhang, X., 2018. Echinacoside increases sperm quantity in rats by targeting the hypothalamic androgen receptor. Sci. Rep. 8, 3839.
Juan, L., Shijun, Y., Zhirui, Y., Wuwen, F., Xintong, M., 2018. Oral hydroxysafflor yellow A reduces obesity in mice by modulating the gut microbiota and serum metabolism. Pharmacol. Res. 134, 40–50.
Kim, Y.S., Ko, B., Kim, D.J., Tak, J., Han, C.Y., Cho, J.-Y., Kim, W., Kim, S.G., 2022. Induction of the hepatic aryl hydrocarbon receptor by alcohol dysregulates autophagy and phospholipid metabolism via PPP2R2D. Nat. Commun. 13, 6080.
Koh, A., Bäckhed, F., 2020. From association to causality: the role of the gut microbiota and its functional products on host metabolism. Mol. Cell. 78, 584–596.
Lamas, B., Richard, M.L., Leducq, V., Pham, H.-P., Michel, M.-L., Da Costa, G., Bridonneau, C., Jegou, S., Hoffmann, T.W., Natividad, J.M., 2016. CARD9 impacts colitis by altering gut microbiota metabolism of tryptophan into aryl hydrocarbon receptor ligands. Nat. Med. 22, 598–605.
Levine, H., Jørgensen, N., Martino-Andrade, A., Mendiola, J., Weksler-Derri, D., Jolles, M., Pinotti, R., Swan, S.H., 2023. Temporal trends in sperm count: a systematic review and meta-regression analysis of samples collected globally in the 20th and 21st centuries. Hum. Reprod. Update. 29, 157–176.
Li, M., Zhao, Y., Wang, Y., Geng, R., Fang, J., Kang, S.G., Huang, K., Tong, T., 2022. Eugenol, a major component of clove oil, attenuates adiposity, and modulates gut microbiota in high-fat diet-fed mice. Mol. Nutr. Food Res. 66, 2200387.

Liu, J.B., Chen, K., Li, Z.F., Wang, Z.Y., Wang, L., 2022. Glyphosate-induced gut microbiota dysbiosis facilitates male reproductive toxicity in rats. Sci. Total Environ. 805, 150368.
Luo, D., Zhang, M., Su, X., Liu, L., Zhou, X., Zhang, X., Zheng, D., Yu, C., Guan, Q., 2020. High fat diet impairs spermatogenesis by regulating glucose and lipid metabolism in Sertoli cells. Life Sci. 257, 118028.
Mruk, D.D., Su, L., Cheng, C.Y., 2011. Emerging role for drug transporters at the blood–testis barrier. Trends Pharmacol. Sci. 32, 99–106.
Muku, G.E., Blazanin, N., Dong, F., Smith, P.B., Thiboutot, D., Gowda, K., Amin, S., Murray, I.A., Perdew, G.H., 2019. Selective Ah receptor ligands mediate enhanced SREBP1 proteolysis to restrict lipogenesis in sebocytes. Toxicol. Sci. 171, 146–158.
Ni, F.D., Hao, S.L., Yang, W.X., 2019. Multiple signaling pathways in Sertoli cells: recent findings in spermatogenesis. Cell Death Dis. 10, 541.
Pohjanvirta, R., 2017. AHR in energy balance regulation. Curr. Opin. Toxicol. 2, 8–14.
Rato, L., Alves, M.G., Socorro, S., Duarte, A.I., Cavaco, J.E., Oliveira, P.F., 2012. Metabolic regulation is important for spermatogenesis. Nat. Rev. Urol. 9, 330–338.
Shi, F., Zhang, Z., Wang, J., Wang, Y., Deng, J., Zeng, Y., Zou, P., Ling, X., Han, F., Liu, J., 2022. Analysis by metabolomics and transcriptomics for the energy metabolism disorder and the aryl hydrocarbon receptor activation in male reproduction of mice and GC-2spd cells exposed to PM2. 5. Front. Endocrinol. 12, 807374.
Shiao, Y.J., Su, M.H., Lin, H.C., Wu, C.R., 2017. Echinacoside ameliorates the memory impairment and cholinergic deficit induced by amyloid beta peptides via the inhibition of amyloid deposition and toxicology. Food Funct. 8, 2283–2294.
Sun, Z.Y., Yu, S., Tian, Y., Han, B.Q., Zhao, Y., Li, Y.Q., Wang, Y., Sun, Y.J., Shen, W., 2022. Chestnut polysaccharides restore impaired spermatogenesis by adjusting gut microbiota and the intestinal structure. Food Funct. 13, 425–436.
Tufek, N.H., Yahyazadeh, A., 2021. Protective effect of indole-3-carbinol on sperm morphometric alteration in a high-fat diet-induced obese rat model. Erciyes Med. J. 43, 161–166.
Wang, J., He, M., Yang, M., Ai, X., 2024. Gut microbiota as a key regulator of intestinal mucosal immunity. Life Sci. 345, 122612.
Wang, M., Ren, C., Wang, P., Cheng, X., Chen, Y., Huang, Y., Chen, J., Sun, Z., Wang, Q., Zhang, Z., 2023a. Microbiome–metabolome reveals the contribution of the gut–testis axis to sperm motility in sheep (Ovis aries). Animals. 13, 996.
Wang, R., Wang, L., Wang, S., Wang, J., Su, C., Zhang, L., Li, C., Liu, S., 2023b. Phenolics from noni (Morinda citrifolia L.) fruit alleviate obesity in high fat diet-fed mice via modulating the gut microbiota and mitigating intestinal damage. Food Chem. 402, 134232.
Wang, Y., Xie, Z., 2022. Exploring the role of gut microbiome in male reproduction. Andrology. 10, 441–450.
Wlodarska, M., Luo, C., Kolde, R., d'Hennezel, E., Annand, J.W., Heim, C.E., Krastel, P., Schmitt, E.K., Omar, A.S., Creasey, E.A., 2017. Indoleacrylic acid produced by commensal peptostreptococcus species suppresses inflammation. Cell Host Microbe. 22 (25–37), e26.
Wu, F., Lei, H., Chen, G., Chen, C., Song, Y., Cao, Z., Zhang, C., Zhang, C., Zhou, J., Lu, Y., 2021. In vitro and in vivo studies reveal that hesperetin-7-o-glucoside, a naturally occurring monoglucoside, exhibits strong anti-inflammatory capacity. J. Agric. Food Chem. 69, 12753–12762.
Wu, D., Wang, T., Liu, H., Xu, F., Xie, S., Tong, X., Li, L., Peng, D., Kong, L., 2023. Wuzi-Yanzong-Wan prevents oligoasthenospermia due to TAp73 suppression by affecting cellular junction remodeling in testicular tissue in mice. J. Ethnopharmacol. 302, 115867.
Xie, J., Yu, J., Zhang, Z., Liu, D., Fan, Y., Wu, Y., Ma, H., Wang, C., Hong, Z., 2022. AMPK pathway is implicated in low level lead-induced pubertal testicular damage via disordered glycolysis. Chemosphere. 291, 132819.
Yan, X., Feng, Y., Hao, Y., Zhong, R., Jiang, Y., Tang, X., Lu, D., Fang, H., Agarwal, M., Chen, L., 2022. Gut-testis axis: microbiota prime metabolome to increase sperm quality in young type 2 diabetes. Microbiol. Spectrum. 10, e01423–e11422.
Yong, S., Yang, Y., Li, F., Yao, H., Yang, F., Chang, D., 2020. Wuzi Yanzong pill for the treatment of male infertility: a protocol for systematic review and meta-analysis of randomized controlled trials. Medicine. 99.
Zhang, P., Feng, Y., Li, L., Ge, W., Yu, S., Hao, Y., Shen, W., Han, X., Ma, D., Yin, S., Tian, Y., Min, L., Sun, Z., Sun, Q., Zhang, H., Zhao, Y., 2021. Improvement in sperm quality and spermatogenesis following faecal microbiota transplantation from alginate oligosaccharide dosed mice. Gut. 70, 222–225.
Zhang, T., Sun, P., Geng, Q., Fan, H., Gong, Y., Hu, Y., Shan, L., Sun, Y., Shen, W., Zhou, Y., 2022. Disrupted spermatogenesis in a metabolic syndrome model: the role of vitamin A metabolism in the gut–testis axis. Gut. 71, 78–87.
Zhao, Q., Dai, M.Y., Huang, R.Y., Duan, J.Y., Zhang, T., Bao, W.M., Zhang, J.Y., Gui, S.Q., Xia, S.M., Dai, C.T., Tang, Y.M., Gonzalez, F.J., Li, F., 2023. Parabacteroides distasonis ameliorates hepatic fibrosis potentially via modulating intestinal bile acid metabolism and hepatocyte pyroptosis in male mice. Nat. Commun. 14, 1829.
Zhao, M.P., Shi, X., Kong, G.W.S., Wang, C.C., Wu, J.C.Y., Lin, Z.X., Li, T.C., Chan, D.Y.L., 2018. The therapeutic effects of a traditional chinese medicine formula wuzi yanzong pill for the treatment of oligoasthenozoospermia: a meta-analysis of randomized controlled trials. Evid. Based Complement. Alternat. Med. 2018, 2968025.
Zierer, J., Jackson, M.A., Kastenmüller, G., Mangino, M., Long, T., Telenti, A., Mohney, R.P., Small, K.S., Bell, J.T., Steves, C.J., Valdes, A.M., Spector, T.D., Menni, C., 2018. The fecal metabolome as a functional readout of the gut microbiome. Nat Genet. 50, 790–795.
Zou, D., Wang, J., Zhang, B., Xie, S., Wang, Q., Xu, K., Lin, R., 2015. Analysis of chemical constituents in Wuzi-Yanzong-Wan by UPLC-ESI-LTQ-Orbitrap-MS. Molecules. 20, 21373–21404.